JACS
JOURNAL OF THE AMERICAN CHEMICAL SOCIETY
pubs.acs.org/JACS
Communication

Hopping Conductance in Molecular Wires Exhibits a Large Heavy-Atom Kinetic Isotope Effect

Quyen Van Nguyen and C. Daniel Frisbie*

Cite This: J. Am. Chem. Soc. 2021, 143, 2638−2643
Read Online
ACCESS | Metrics & More | Article Recommendations | Supporting Information

ABSTRACT: We report a large kinetic isotope effect (KIE) for intramolecular charge transport in π-conjugated oligophenyleneimine (OPI) molecules connected to Au electrodes. ^{13}C and ^{15}N substitution on the imine bonds produces a conductance KIE of ∼2.7 per labeled atom in long OPI wires >4 nm in length, far larger than typical heavy-atom KIEs for chemical reactions. In contrast, isotopic labeling in shorter OPI wires <4 nm does not produce a conductance KIE, consistent with a direct tunneling mechanism. Temperature-dependent measurements reveal that conductance for a long ^{15}N-substituted OPI wire is activated, and we propose that the exceptionally large conductance KIEs imply a thermally assisted, through-barrier polaron tunneling mechanism. In general, observation of large conductance KIEs opens up considerable opportunities for understanding microscopic conduction mechanisms in π-conjugated molecules.

The use of isotopic labeling to examine electrical conduction mechanisms in molecular conductors is relatively rare,[1−3] perhaps because the effects have generally been expected to be quite small. In principle, however, exploration of conduction isotope effects in molecular systems holds promise for deciphering charge transport mechanisms,[4−6] including rate-limiting steps and transition states, in exact analogy with the study of kinetic isotope effects (KIEs) for determining reaction mechanisms in physical organic chemistry.

Here we report the discovery of a large KIE for hopping conduction in nanoscopic π-conjugated molecular wires connected between Au electrodes. Our experiments focus on ^{13}C-, ^{15}N-, and D-labeled oligophenyleneimine (OPI) wires grown from Au substrates, Figure 1A (see also Figures S1−S3 in the Supporting Information), with the number of phenylenes in the range n = 2−10, corresponding to molecular lengths of 1−7 nm. Figure 1A shows that our labeling studies to date have focused on the imine linkage (−C(H)═N−). The OPI wires are synthesized on Au surfaces beginning with formation of self-assembled monolayers (SAMs) of 4-aminothiophenol followed by sequential "click-like" condensation reactions with aryl dialdehydes and diamines, as we have reported previously.[7−10] Isotopic substitution is achieved by using monomers shown in Figure 1B. Monomers **1**, **2**, and **7**−**10** are commercially available, and **3**−**6** were synthesized as described in the Supporting Information. The syntheses of 27 different ^{13}C-, ^{15}N-, and D-substituted OPI wires and 9 unsubstituted versions, along with their characterization by infrared and X-ray photoelectron spectroscopies, are reported in Figures S4−S9 in the Supporting Information.

To measure the conductance (or resistance) of the isotopically substituted OPI wires, we employed the conducting probe atomic force microscopy (CP-AFM) platform, Figure 2A.[7,9−15] Au-coated probe tips were brought into soft (∼1 nN) contact with the OPI wire films, and voltage was

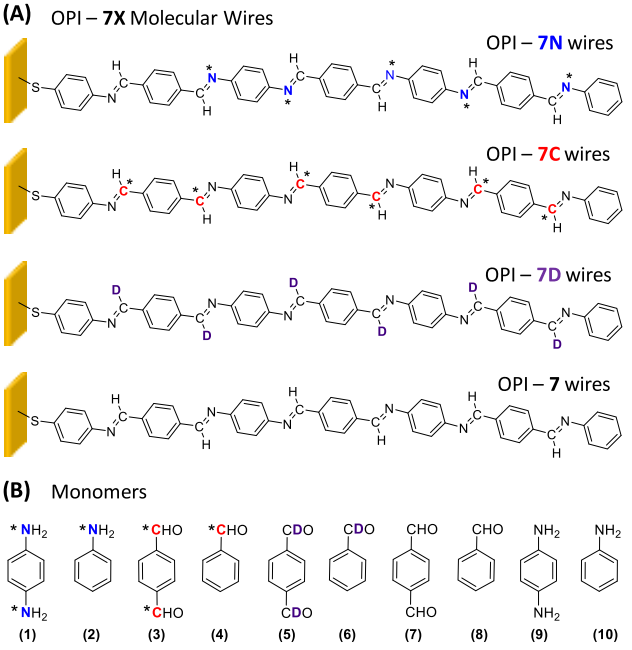

Figure 1. (a) Structures of isotopologues OPI-7N, OPI-7C, OPI-7D, and the unsubstituted OPI-7 parent molecule on Au. The general naming scheme is OPI-nX, where n = 2−10 is the number of phenylene rings and X is the isotope. (b) Corresponding monomer units used to synthesize the OPI wires. * denotes ^{15}N or ^{13}C.

Received: November 23, 2020
Published: February 15, 2021

https://dx.doi.org/10.1021/jacs.0c12244
J. Am. Chem. Soc. 2021, 143, 2638−2643

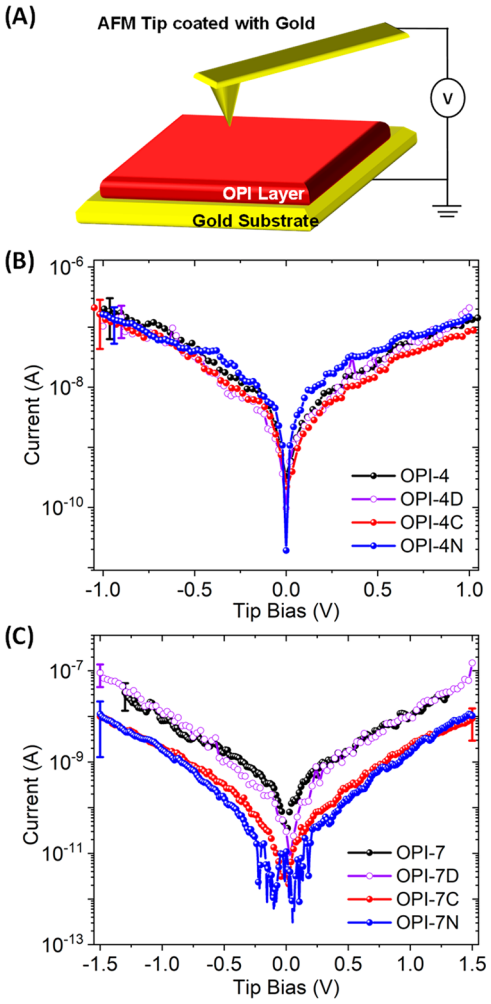

Figure 2. (a) Scheme of the CP-AFM setup. (b) Semilog plots of averaged $I-V$ curves for OPI-4 and OPI-4X. (c) Averaged $I-V$ curves for OPI-7 and OPI-7X. Each curve is the average of 200 $I-V$ traces. The error bars represent one standard deviation.

swept at the tip while the substrate was grounded. Figure 2B displays the resulting current−voltage ($I-V$) characteristics on a semi-log scale for OPI-4 and the ^{13}C-, ^{15}N-, and D-labeled versions, OPI-4C, OPI-4N, and OPI-4D, respectively. Differences in average currents are within the error of the measurements, and there is no apparent KIE. We have established previously that, for short OPI molecules up to OPI-5, the dominant electrical transport mechanism is direct tunneling,[7,9,10,12] and in such a situation, a significant KIE is not expected.

Figure 2C reveals a very different result for the longer oligomers OPI-7, OPI-7C, and OPI-7N. The ^{13}C- and ^{15}N-substituted OPI-7C and OPI-7N molecules have significantly lower current than OPI-7, by about a factor of 3−5, at all voltages. Similar observations hold for n = 6 and longer (n = 8−10) ^{13}C- and ^{15}N-substituted wires, Figures S10−S12. However, there is no apparent difference in currents for OPI-7D versus OPI-7. In prior work, we have demonstrated that the mechanism of charge transport in long OPI wires is thermally activated, multistep hopping in which holes are injected into the OPI π-systems and driven along the molecules by the applied electric field.[7,9,10,12] The localized hole is best described as a polaron, i.e., charge and the accompanying geometric distortion of bond lengths and angles in the molecular backbone, Scheme 1. In this situation, transition

Scheme 1. Representation of a Polaron in an OPI Oligomer

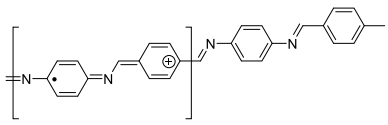

state theory applies for each intramolecular polaron hop and one expects a KIE.[16−25] Our observations of KIEs in long molecules (n = 6−10) are consistent with this expectation.

Low bias resistance versus molecular length results for all 36 OPI wires are shown in Figure 3A. The tunneling and hopping

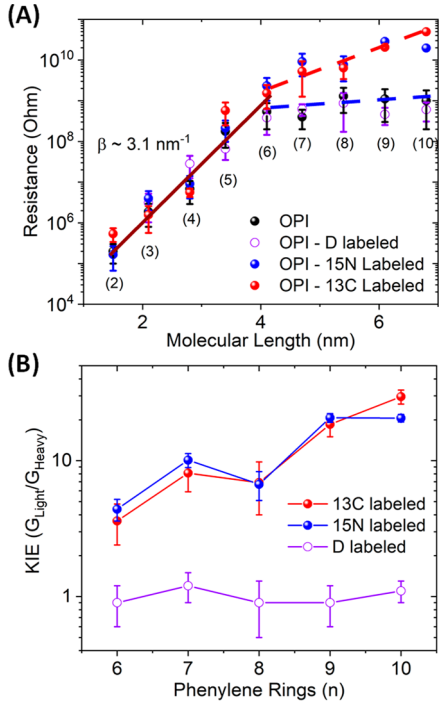

Figure 3. (a) Semi-log plot of low bias (±0.5 V) resistance versus molecular length. Corresponding ring numbers are indicated. Error bars are one standard deviation. Each point represents the average of 200 $I-V$ traces. (b) KIEs for labeled OPI wires versus ring number extracted from the data in (a).

transport regimes are defined by the stark slope change evident in the resistance data. For short OPI molecules below 4 nm in which direct tunneling dominates, the resistance increases exponentially with molecular length, as expected.[7,9,10,12,26−33] There is no KIE in this regime for any of the wires; the resistance versus length behavior is indistinguishable for the labeled versus unlabeled versions. For long OPI wires >4 nm where the transport mechanism is polaron hopping, large KIEs are evident. In particular, the ^{13}C- and ^{15}N-substituted wires have distinctly higher resistances (R) than the unlabeled OPI wires. The slopes of the R vs length trends are also steeper for the ^{13}C and ^{15}N isotopologues. H/D exchange on the imine functionality did not produce a KIE for any OPI wire length.

Conductance KIEs are quantified by the ratio of wire conductances G (= $1/R$), which are directly proportional to polaron hopping rates, i.e., KIE = G_{light}/G_{heavy} = R_{heavy}/R_{light}, where G_{light} (R_{light}) is the conductance (resistance) of the

https://dx.doi.org/10.1021/jacs.0c12244
J. Am. Chem. Soc. 2021, 143, 2638−2643

Table 1. Summary of the Kinetic Isotopic Effect for Labeled OPI Wires[a]

Ring Number	^{13}C	KIE per ^{13}C	^{15}N	KIE per ^{15}N	D
6	3.6 ± 1.2	0.7 ± 0.2	4.4 ± 0.8	1.1 ± 0.2	0.9 ± 0.3
7	8.1 ± 2.2	1.4 ± 0.4	10.1 ± 1.2	2.0 ± 0.2	1.2 ± 0.3
8	6.9 ± 2.9	1.0 ± 0.4	6.7 ± 1.6	1.2 ± 0.3	0.9 ± 0.4
9	18.5 ± 3.5	**2.3 ± 0.4**	20.7 ± 1.5	**2.9 ± 0.2**	0.9 ± 0.3
10	29.6 ± 3.5	**3.3 ± 0.4**	20.6 ± 2.5	**2.5 ± 0.3**	1.1 ± 0.2

[a]KIE = $G_{light}/G_{heavy} = R_{heavy}/R_{light}$. KIE per ^{13}C/^{15}N is the KIE divided by the number of heavy isotope atoms per wire.

unlabeled molecule and G_{heavy} (R_{heavy}) corresponds to the heavy-atom isotopologue. For all ^{13}C- and ^{15}N-substituted wires in the hopping regime, KIE ≫ 1, as shown in Figure 3B and Table 1. These conductance KIEs are exceptionally large, ranging from 3 to 30. Primary KIEs for reactions involving ^{13}C-labeled molecules, and to a lesser extent ^{15}N-isotopologues, are documented in solution- and gas-phase studies and are generally quite small (^{13}C KIE < 1.01) near room temperature.[34−39] However, unlike typical reaction kinetics studies in which single bond breaking or formation rates are the primary focus, the conductance KIEs reported here represent an aggregate of multiple intramolecular polaron transfer events, involving many bonds in the wire backbone.

To normalize the KIEs, we divided the total KIE for each wire by the number of isotope atoms present in the wire (e.g., n − 1 isotope atoms for OPI-nC wires). The isotope normalized KIEs are also shown in Table 1 and range from 0.7 to 3.3, generally increasing with length. We believe the isotope normalized KIEs for the longest wires (highlighted in bold in Table 1) are more reliable than those for the n = 6−8 wires, for two reasons. First, there will be more polaron hopping events in the longest wires and hence a greater number of labeled imine bonds will be sampled. Second, it seems quite likely there are "end-effects" in the conductance measurements that impact the calculation of the normalized KIE. For example, the normalized KIE for the OPI-6C wires is 0.7 (Table 1), which suggests a rate *increase* compared to the unlabeled OPI-6, but this is at odds with the total KIE for OPI-6C wires that shows they are 3.6× more resistive than unlabeled OPI-6 wires. This discrepancy is resolved if one presumes that imine bonds closest to the contacts somehow do not contribute to the wire resistance, perhaps because injected charge is initially distributed over several rings. The upshot is that we take the normalized KIEs for OPI-9C, OPI-9N, OPI-10C, and OPI-10N in Table 1 as better values. The approximate mean normalized KIE for these wires is 2.7, which again is an extraordinarily large value compared to typical heavy atom KIEs in chemistry.

Prior quantum chemical calculations by Gagliardi, Cramer, and co-workers for isolated, positively charged OPI wires revealed that the polaron is localized to a few repeat units such that multiple hops are necessary to traverse the entire wire length.[9,10] These calculations also indicated that the intramolecular hopping transition states involve simultaneous flattening of the dihedral angle between adjacent phenylenes and lengthening of the −C═N− (imine) bond. In this scenario, the substitution of heavy isotopes in the imine linkage is expected to produce a KIE as the ground state vibration frequency is decreased, leading to a higher barrier and fewer attempted crossings through the transition state per unit time. Understanding the role of intermolecular interactions on the transition state is important, as is whether ^{13}C exchange in the phenyl rings has an impact similar to labeling the imine functionality. Those studies are ongoing. Likewise, there are fluctuations in KIE with increasing n, and further investigation is necessary to determine the cause. Nevertheless, our current observations verify the key role of the imine bond on the polaron hopping rate.

The critical question is why the observed conductance KIEs are so large. Computational estimates of the transition state energies for polaron hopping in OPIs are ∼100 meV (10 kJ/mol) corresponding to concurrent bond stretching and torsional ring motion. Indeed, we have made initial temperature-dependent measurements that reveal conductance activation energies of 200−300 meV for both OPI-7N and OPI-7 (Figure S13), and it does not appear that activation energy differences can explain the large ^{15}N KIE at room temperature (Table 1). Furthermore, while heavy atom substitution will decrease the barrier attempt frequency, the small percentage increases in atomic weights for ^{13}C and ^{15}N substitution are unable to account for the large KIEs. This suggested to us that a classical over-the-barrier mechanism may be inadequate to explain the large KIEs for intramolecular polaron transport.

An intriguing possibility is that the transport mechanism involves thermally assisted polaron tunneling.[18,40−44] By polaron tunneling we mean coupled charge and nuclear (e.g., C, N) tunneling, i.e., a simultaneous change in both electronic and nuclear coordinates. Generally speaking, observation of exceptionally large KIEs can be an indicator of nuclear tunneling processes.[45−50] Nuclear tunneling is known to play a critical role in the bond shift isomerization of cyclobutadiene[47,51−53] and the umbrella inversion of the ammonia molecule,[47,54−56] for example, as well as other reactions.[34,36−39,47,57−59] Other authors have also proposed a role for ^{12}C-tunneling in polaron transport in molecular semiconductors.[40−44] For the OPI system, the conditions for nuclear tunneling appear to be met, namely a small barrier height (∼100 meV) and a narrow barrier width. The narrow barrier width is inferred from the polaron hopping transition state, which involves stretching of the imine bond. Changing the imine bond order from two (C═N) to one (C−N), as implied by the change from aromatic to quinoidal bonding patterns in OPI polarons,[7,9,10] results in a bond length increase of only ∼0.2 Å, supporting the narrow barrier concept.

For a thermally assisted polaron tunneling mechanism, a crucial question is whether the estimated nuclear tunneling rates are compatible with the rate of charge transfer through the OPI molecules. A second question is whether large KIEs can indeed be predicted, even approximately. Inspection of Figure 2 shows that current levels of 1 nA pass through the metal-OPI-7-metal junctions at V = 0.5 V. From prior work we know that 50−100 OPI-7 molecules are contacted by the CP-AFM probe.[8,13,60] To make a conservative calculation, we assume that the current passes through on average 10 OPI-7 molecules. This corresponds to 10^9 holes/s per molecule, or a

https://dx.doi.org/10.1021/jacs.0c12244
J. Am. Chem. Soc. 2021, 143, 2638−2643

hole transit time per molecule of approximately 1 ns. Approximate rates of nuclear tunneling can be calculated as outlined by Karmakar and Datta in their recent paper on heavy atom tunneling in organic reactions.[47] Assuming a parabolic barrier for ^{12}C atom tunneling that is 100 meV in height and 0.2 Å in width, gives a transmission probability $T = 5 \times 10^{-4}$. Multiplying T by the C═N vibration frequency of 5×10^{13} s^{-1} (~1600 cm^{-1}), we obtain a ^{12}C-tunneling rate of 10^{10} s^{-1}, an extraordinarily large value. Importantly, this tunneling rate is compatible with (faster than) the estimated 10^{9} s^{-1} rate of hole transfer across the OPI molecules at $V = 0.5$ V. A similar calculation for ^{13}C-tunneling gives $T = 3.7 \times 10^{-4}$, yielding a KIE = 1.4 for a single labeled imine bond. This estimated KIE appears to be within a factor of 2 of our normalized KIE/isotope (~2.7), and thus is in reasonable agreement given the approximate nature of the calculation.

In summary, we have discovered extraordinarily large heavy atom KIEs for intramolecular charge transport in π-conjugated oligomers. The results may be consistent with a thermally assisted, intramolecular polaron tunneling mechanism. Further experiments, for example conductance measurements down to much lower temperatures (e.g., 10 K) where activated processes freeze out and tunneling processes dominate, are desirable.[4,18,40,42,44] Additionally, computational analysis will be essential for assessment of the role of nuclear tunneling and for obtaining quantitative agreement between transport experiments and theory, especially in light of the large electric fields involved, which alter the potential energy landscape. It seems clear that the discovery of large heavy-atom KIEs for intramolecular polaron transport—independent of whether heavy-atom tunneling is occurring—opens up opportunities for understanding microscopic conduction mechanisms in molecules. If polaron tunneling effects are confirmed, intramolecular charge transport experiments may also provide a platform for examination of heavy-atom tunneling processes generally.

■ ASSOCIATED CONTENT

Supporting Information

The Supporting Information is available free of charge at https://pubs.acs.org/doi/10.1021/jacs.0c12244.

Chemical structures of all OPI wires, details of OPI wire synthesis and monomer synthesis, reflection–absorption infrared spectra (RAIRS), X-ray photoelectron spectra (XPS), experimental details on transport measurements, and I–V curves of all labeled OPI wires (PDF)

■ AUTHOR INFORMATION

Corresponding Author

C. Daniel Frisbie − *Department of Chemical Engineering and Materials Science, University of Minnesota, Minneapolis, Minnesota 55455, United States;* orcid.org/0000-0002-4735-2228; Email: frisbie@umn.edu

Author

Quyen Van Nguyen − *Department of Chemical Engineering and Materials Science, University of Minnesota, Minneapolis, Minnesota 55455, United States;* orcid.org/0000-0003-0120-0971

Complete contact information is available at: https://pubs.acs.org/10.1021/jacs.0c12244

Notes

The authors declare no competing financial interest.

■ ACKNOWLEDGMENTS

The authors acknowledge the financial support of the National Science Foundation (CHE-2003199). Parts of this work were carried out in the Characterization Facility, University of Minnesota, which receives partial support from the NSF through the MRSEC (Award Number DMR-2011401) and NNCI programs (Award Number ECCS-2025124).

■ REFERENCES

(1) Carlson, K. D.; Williams, J. M.; Geiser, U.; Kini, A. M.; Wang, H. H.; Klemm, R. A.; Kumar, S. K.; Schlueter, J. A.; Ferraro, J. R. The central bond ^{13}C═^{13}C isotope effect for superconductivity in high-Tc β-$(ET)_2I_3$ and its implications regarding the superconducting pairing mechanism. *J. Am. Chem. Soc.* **1992**, *114* (25), 10069–10071.

(2) Kato, R.; Aonuma, S.; Sawa, H.; Hiraki, K.; Takahashi, T. Unexpected isotope effect in ^{13}C-substituted (−C ≡ N) molecular conductor (DMe-DCNQI)2Cu (DMe-DCNQI = 2,5-dimethyl-N,N′-dicyanoquinone-diimine). *Synth. Met.* **1995**, *68* (2), 195–198.

(3) Ren, X.; Bruzek, M. J.; Hanifi, D. A.; Schulzetenberg, A.; Wu, Y.; Kim, C.-H.; Zhang, Z.; Johns, J. E.; Salleo, A.; Fratini, S.; Troisi, A.; Douglas, C. J.; Frisbie, C. D. Negative Isotope Effect on Field-Effect Hole Transport in Fully Substituted ^{13}C-Rubrene. *Adv. Electron. Mater.* **2017**, *3* (4), 1700018.

(4) Amdursky, N.; Pecht, I.; Sheves, M.; Cahen, D. Marked changes in electron transport through the blue copper protein azurin in the solid state upon deuteration. *Proc. Natl. Acad. Sci. U. S. A.* **2013**, *110* (2), 507.

(5) Amdursky, N.; Sepunaru, L.; Raichlin, S.; Pecht, I.; Sheves, M.; Cahen, D. Electron Transfer Proteins as Electronic Conductors: Significance of the Metal and Its Binding Site in the Blue Cu Protein, Azurin. *Adv. Sci.* **2015**, *2* (4), 1400026.

(6) Chen, X.; Salim, T.; Zhang, Z.; Yu, X.; Volkova, I.; Nijhuis, C. A. Large Increase in the Dielectric Constant and Partial Loss of Coherence Increases Tunneling Rates across Molecular Wires. *ACS Appl. Mater. Interfaces* **2020**, *12* (40), 45111–45121.

(7) Ho Choi, S.; Kim, B.; Frisbie, C. D. Electrical Resistance of Long Conjugated Molecular Wires. *Science* **2008**, *320* (5882), 1482.

(8) Demissie, A. T.; Haugstad, G.; Frisbie, C. D. Growth of Thin, Anisotropic, π-Conjugated Molecular Films by Stepwise "Click" Assembly of Molecular Building Blocks: Characterizing Reaction Yield, Surface Coverage, and Film Thickness versus Addition Step Number. *J. Am. Chem. Soc.* **2015**, *137* (27), 8819–8828.

(9) Smith, C. E.; Odoh, S. O.; Ghosh, S.; Gagliardi, L.; Cramer, C. J.; Frisbie, C. D. Length-Dependent Nanotransport and Charge Hopping Bottlenecks in Long Thiophene-Containing π-Conjugated Molecular Wires. *J. Am. Chem. Soc.* **2015**, *137* (50), 15732–15741.

(10) Taherinia, D.; Smith, C. E.; Ghosh, S.; Odoh, S. O.; Balhorn, L.; Gagliardi, L.; Cramer, C. J.; Frisbie, C. D. Charge Transport in 4 nm Molecular Wires with Interrupted Conjugation: Combined Experimental and Computational Evidence for Thermally Assisted Polaron Tunneling. *ACS Nano* **2016**, *10* (4), 4372–4383.

(11) Rodriguez-Gonzalez, S.; Xie, Z.; Galangau, O.; Selvanathan, P.; Norel, L.; Van Dyck, C.; Costuas, K.; Frisbie, C. D.; Rigaut, S.; Cornil, J. HOMO Level Pinning in Molecular Junctions: Joint Theoretical and Experimental Evidence. *J. Phys. Chem. Lett.* **2018**, *9* (9), 2394–2403.

(12) Sangeeth, C. S. S.; Demissie, A. T.; Yuan, L.; Wang, T.; Frisbie, C. D.; Nijhuis, C. A. Comparison of DC and AC Transport in 1.5–7.5 nm Oligophenylene Imine Molecular Wires across Two Junction Platforms: Eutectic Ga–In versus Conducting Probe Atomic Force Microscope Junctions. *J. Am. Chem. Soc.* **2016**, *138* (23), 7305–7314.

(13) Xie, Z.; Bâldea, I.; Demissie, A. T.; Smith, C. E.; Wu, Y.; Haugstad, G.; Frisbie, C. D. Exceptionally Small Statistical Variations in the Transport Properties of Metal–Molecule–Metal Junctions

Composed of 80 Oligophenylene Dithiol Molecules. *J. Am. Chem. Soc.* **2017**, *139* (16), 5696−5699.
(14) Xie, Z.; Bâldea, I.; Frisbie, C. D. Determination of Energy-Level Alignment in Molecular Tunnel Junctions by Transport and Spectroscopy: Self-Consistency for the Case of Oligophenylene Thiols and Dithiols on Ag, Au, and Pt Electrodes. *J. Am. Chem. Soc.* **2019**, *141* (8), 3670−3681.
(15) Xie, Z.; Bâldea, I.; Frisbie, C. D. Energy Level Alignment in Molecular Tunnel Junctions by Transport and Spectroscopy: Self-Consistency for the Case of Alkyl Thiols and Dithiols on Ag, Au, and Pt Electrodes. *J. Am. Chem. Soc.* **2019**, *141* (45), 18182−18192.
(16) Coropceanu, V.; Cornil, J.; da Silva Filho, D. A.; Olivier, Y.; Silbey, R.; Brédas, J.-L. Charge Transport in Organic Semiconductors. *Chem. Rev.* **2007**, *107* (4), 926−952.
(17) Oberhofer, H.; Reuter, K.; Blumberger, J. Charge Transport in Molecular Materials: An Assessment of Computational Methods. *Chem. Rev.* **2017**, *117* (15), 10319−10357.
(18) Jiang, Y.; Geng, H.; Li, W.; Shuai, Z. Understanding Carrier Transport in Organic Semiconductors: Computation of Charge Mobility Considering Quantum Nuclear Tunneling and Delocalization Effects. *J. Chem. Theory Comput.* **2019**, *15* (3), 1477−1491.
(19) Nitzan, A. Electron Transmission Through Molecules and Molecular Interfaces. *Annu. Rev. Phys. Chem.* **2001**, *52* (1), 681−750.
(20) Nitzan, A.; Ratner, M. A. Electron Transport in Molecular Wire Junctions. *Science* **2003**, *300* (5624), 1384.
(21) Galperin, M.; Ratner, M. A.; Nitzan, A. Molecular transport junctions: vibrational effects. *J. Phys.: Condens. Matter* **2007**, *19* (10), 103201.
(22) Galperin, M.; Ratner, M. A.; Nitzan, A. Hysteresis, Switching, and Negative Differential Resistance in Molecular Junctions: A Polaron Model. *Nano Lett.* **2005**, *5* (1), 125−130.
(23) Galperin, M.; Ratner, M. A.; Nitzan, A.; Troisi, A. Nuclear Coupling and Polarization in Molecular Transport Junctions: Beyond Tunneling to Function. *Science* **2008**, *319* (5866), 1056.
(24) Luo, L.; Choi, S. H.; Frisbie, C. D. Probing Hopping Conduction in Conjugated Molecular Wires Connected to Metal Electrodes. *Chem. Mater.* **2011**, *23* (3), 631−645.
(25) Joachim, C.; Ratner, M. A. Molecular electronics: Some views on transport junctions and beyond. *Proc. Natl. Acad. Sci. U. S. A.* **2005**, *102* (25), 8801.
(26) Tefashe, U. M.; Nguyen, Q. V.; Lafolet, F.; Lacroix, J.-C.; McCreery, R. L. Robust Bipolar Light Emission and Charge Transport in Symmetric Molecular Junctions. *J. Am. Chem. Soc.* **2017**, *139* (22), 7436−7439.
(27) Nguyen, Q. V.; Martin, P.; Frath, D.; Della Rocca, M. L.; Lafolet, F.; Bellinck, S.; Lafarge, P.; Lacroix, J.-C. Highly Efficient Long-Range Electron Transport in a Viologen-Based Molecular Junction. *J. Am. Chem. Soc.* **2018**, *140* (32), 10131−10134.
(28) Nguyen, Q. V.; Tefashe, U.; Martin, P.; Della Rocca, M. L.; Lafolet, F.; Lafarge, P.; McCreery, R. L.; Lacroix, J.-C. Molecular Signature and Activationless Transport in Cobalt-Terpyridine-Based Molecular Junctions. *Adv. Electron. Mater.* **2020**, *6* (7), 1901416.
(29) Hines, T.; Diez-Perez, I.; Hihath, J.; Liu, H.; Wang, Z.-S.; Zhao, J.; Zhou, G.; Müllen, K.; Tao, N. Transition from Tunneling to Hopping in Single Molecular Junctions by Measuring Length and Temperature Dependence. *J. Am. Chem. Soc.* **2010**, *132* (33), 11658−11664.
(30) Xiang, D.; Wang, X.; Jia, C.; Lee, T.; Guo, X. Molecular-Scale Electronics: From Concept to Function. *Chem. Rev.* **2016**, *116* (7), 4318−4440.
(31) Bowers, C. M.; Rappoport, D.; Baghbanzadeh, M.; Simeone, F. C.; Liao, K.-C.; Semenov, S. N.; Żaba, T.; Cyganik, P.; Aspuru-Guzik, A.; Whitesides, G. M. Tunneling across SAMs Containing Oligophenyl Groups. *J. Phys. Chem. C* **2016**, *120* (21), 11331−11337.
(32) Yan, H.; Bergren, A. J.; McCreery, R.; Della Rocca, M. L.; Martin, P.; Lafarge, P.; Lacroix, J. C. Activationless charge transport across 4.5 to 22 nm in molecular electronic junctions. *Proc. Natl. Acad. Sci. U. S. A.* **2013**, *110* (14), 5326.
(33) Karuppannan, S. K.; Neoh, E. H. L.; Vilan, A.; Nijhuis, C. A. Protective Layers Based on Carbon Paint To Yield High-Quality Large-Area Molecular Junctions with Low Contact Resistance. *J. Am. Chem. Soc.* **2020**, *142* (7), 3513−3524.
(34) Gómez-Gallego, M.; Sierra, M. A. Kinetic Isotope Effects in the Study of Organometallic Reaction Mechanisms. *Chem. Rev.* **2011**, *111* (8), 4857−4963.
(35) Phillips, L. M.; Lee, J. K. Theoretical Studies of Mechanisms and Kinetic Isotope Effects on the Decarboxylation of Orotic Acid and Derivatives. *J. Am. Chem. Soc.* **2001**, *123* (48), 12067−12073.
(36) Gable, K. P.; Zhuravlev, F. A. Kinetic Isotope Effects in Cycloreversion of Rhenium (V) Diolates. *J. Am. Chem. Soc.* **2002**, *124* (15), 3970−3979.
(37) Snider, M. J.; Reinhardt, L.; Wolfenden, R.; Cleland, W. W. 15N Kinetic Isotope Effects on Uncatalyzed and Enzymatic Deamination of Cytidine. *Biochemistry* **2002**, *41* (1), 415−421.
(38) Christian, C. F.; Takeya, T.; Szymanski, M. J.; Singleton, D. A. Isotope Effects and the Mechanism of Epoxidation of Cyclohexenone with tert-Butyl Hydroperoxide. *J. Org. Chem.* **2007**, *72* (16), 6183−6189.
(39) Feilberg, K. L.; Gruber-Stadler, M.; Johnson, M. S.; Mühlhäuser, M.; Nielsen, C. J. 13C, 18O, and D Fractionation Effects in the Reactions of CH3OH Isotopologues with Cl and OH Radicals. *J. Phys. Chem. A* **2008**, *112* (44), 11099−11114.
(40) Jiang, Y.; Geng, H.; Shi, W.; Peng, Q.; Zheng, X.; Shuai, Z. Theoretical Prediction of Isotope Effects on Charge Transport in Organic Semiconductors. *J. Phys. Chem. Lett.* **2014**, *5* (13), 2267−2273.
(41) Jiang, Y.; Peng, Q.; Geng, H.; Ma, H.; Shuai, Z. Negative isotope effect for charge transport in acenes and derivatives − a theoretical conclusion. *Phys. Chem. Chem. Phys.* **2015**, *17* (5), 3273−3280.
(42) Jiang, Y.; Zhong, X.; Shi, W.; Peng, Q.; Geng, H.; Zhao, Y.; Shuai, Z. Nuclear quantum tunnelling and carrier delocalization effects to bridge the gap between hopping and bandlike behaviors in organic semiconductors. *Nanoscale Horiz.* **2016**, *1* (1), 53−59.
(43) van der Kaap, N. J.; Katsouras, I.; Asadi, K.; Blom, P. W. M.; Koster, L. J. A.; de Leeuw, D. M., Charge transport in disordered semiconducting polymers driven by nuclear tunneling. *Phys. Rev. B* **2016**, *93* (14). DOI: 10.1103/PhysRevB.93.140206.
(44) Asadi, K.; Kronemeijer, A. J.; Cramer, T.; Jan Anton Koster, L.; Blom, P. W. M.; de Leeuw, D. M. Polaron hopping mediated by nuclear tunnelling in semiconducting polymers at high carrier density. *Nat. Commun.* **2013**, *4* (1), 1710.
(45) Marcus, R. A., Electron and Nuclear Tunneling in Chemical and Biological Systems. In *Tunneling in Biological Systems*; Chance, B., Marcus, R. A., Devault, D. C., Schrieffer, J. R., Frauenfelder, H., Sutin, N., Eds.; Academic Press: 1979; pp 109−127.
(46) Meisner, J.; Kästner, J. Atom Tunneling in Chemistry. *Angew. Chem., Int. Ed.* **2016**, *55* (18), 5400−5413.
(47) Karmakar, S.; Datta, A. Heavy-atom tunneling in organic transformations. *J. Chem. Sci.* **2020**, *132* (1), 127.
(48) Nakanishi, I.; Shoji, Y.; Ohkubo, K.; Ozawa, T.; Matsumoto, K.-i.; Fukuzumi, S. A large kinetic isotope effect in the reaction of ascorbic acid with 2-phenyl-4,4,5,5-tetramethylimidazoline-1-oxyl 3-oxide (PTIO˙) in aqueous buffer solutions. *Chem. Commun.* **2020**, *56* (77), 11505−11507.
(49) Schreiner, P. R. Quantum Mechanical Tunneling Is Essential to Understanding Chemical Reactivity. *Trends Chem.* **2020**, *2* (11), 980−989.
(50) Castro, C.; Karney, W. L. Heavy-Atom Tunneling in Organic Reactions. *Angew. Chem., Int. Ed.* **2020**, *59* (22), 8355−8366.
(51) Carpenter, B. K. Heavy-atom tunneling as the dominant pathway in a solution-phase reaction? Bond shift in antiaromatic annulenes. *J. Am. Chem. Soc.* **1983**, *105* (6), 1700−1701.
(52) Schoonmaker, R.; Lancaster, T.; Clark, S. J. Quantum mechanical tunneling in the automerization of cyclobutadiene. *J. Chem. Phys.* **2018**, *148* (10), 104109.

https://dx.doi.org/10.1021/jacs.0c12244
J. Am. Chem. Soc. 2021, 143, 2638−2643

(53) Huang, M. J.; Wolfsberg, M. Tunneling in the automerization of cyclobutadiene. *J. Am. Chem. Soc.* **1984**, *106* (14), 4039−4040.
(54) Park, Y.; Kang, H.; Field, R. W.; Kang, H. The frequency-domain infrared spectrum of ammonia encodes changes in molecular dynamics caused by a DC electric field. *Proc. Natl. Acad. Sci. U. S. A.* **2019**, *116* (47), 23444.
(55) Dennison, D. M.; Uhlenbeck, G. E. The Two-Minima Problem and the Ammonia Molecule. *Phys. Rev.* **1932**, *41* (3), 313−321.
(56) Rauk, A.; Allen, L. C.; Mislow, K. Pyramidal Inversion. *Angew. Chem., Int. Ed. Engl.* **1970**, *9* (6), 400−414.
(57) Michel, C. S.; Lampkin, P. P.; Shezaf, J. Z.; Moll, J. F.; Castro, C.; Karney, W. L. Tunneling by 16 Carbons: Planar Bond Shifting in [16]Annulene. *J. Am. Chem. Soc.* **2019**, *141* (13), 5286−5293.
(58) Ertelt, M.; Hrovat, D. A.; Borden, W. T.; Sander, W. Heavy-atom tunneling in the ring opening of a strained cyclopropene at very low temperatures. *Chem. - Eur. J.* **2014**, *20* (16), 4713−20.
(59) Zuev, P. S.; Sheridan, R. S.; Albu, T. V.; Truhlar, D. G.; Hrovat, D. A.; Borden, W. T. Carbon Tunneling from a Single Quantum State. *Science* **2003**, *299* (5608), 867.
(60) Demissie, A. T.; Haugstad, G.; Frisbie, C. D. Quantitative Surface Coverage Measurements of Self-Assembled Monolayers by Nuclear Reaction Analysis of Carbon-12. *J. Phys. Chem. Lett.* **2016**, *7* (17), 3477−3481.

https://dx.doi.org/10.1021/jacs.0c12244
J. Am. Chem. Soc. 2021, 143, 2638−2643